Influence of wavelength on nonadiabatic effects in circularly polarized strong-field ionization

MingHu Yuan,[1] GuangJiu Zhao,[1,2] and HongPing Liu[1,*]

[1]*State Key Laboratory of Magnetic Resonances and Atomic and Molecular Physics, Wuhan Institute of Physics and Mathematics, Chinese Academy of Sciences, Wuhan 430071, China*

[2]*State Key Laboratory of Molecular Reaction Dynamics, Dalian Institute of Chemical Physics, Chinese Academy of Sciences, Dalian 116023, China*

(Received 16 July 2015; published 5 November 2015)

The influence of wavelength on nonadiabatic effects in an intensive, circularly polarized laser field has been studied by solving the time-dependent Schrödinger equation of a single active electron of the argon atom in a three-dimensional spherical coordinate system. The nonadiabatic process considering the nonzero initial velocity of the electron is very vital to reproducing the experimental observation. Our calculated photoelectron angular distribution in the directions perpendicular to the polarization plane shows nonadiabatic effects in strong laser ionization. The analysis of angular distribution on the "fast" time scale corresponding to wavelength indicates that as the wavelength gets shorter, the nonadiabatic effects get stronger. While the analysis on the "slow" time scale corresponding to the pulse envelope shows that the short pulse duration comes to play an important role for the nonadiabatic effects. When the pulse duration is more than 15 cycles, the influence of pulse duration on nonadiabatic effects fades away and the effects approach stabilization.

DOI: 10.1103/PhysRevA.92.053405 PACS number(s): 32.80.Fb, 31.15.ac, 32.80.Rm

I. INTRODUCTION

In atomic and molecular physics, strong laser field ionization under certain conditions is described by a tunneling process which is one of the primary manifestations of quantum mechanics departing from classical physics. In this process, the laser field bends the binding Coulomb potential of an atom or molecule forming a barrier through which the electron may tunnel out without gaining any energy [1]. When the laser field is weak enough, multiphoton absorption may occur, where the electron escapes from the bound state by absorbing multiple photons [2]. The two regimes are usually distinguished by the Keldysh parameter $\gamma = \omega\sqrt{2I_{\rm ion}(\varepsilon^2+1)}/F_0$, where $I_{\rm ion}$ is the ionization potential, F_0 is the peak intensity of the laser electric field, ε is the ellipticity, and ω is the laser angular frequency [3]. Unless otherwise stated, atomic units are utilized. In the tunneling regime where $\gamma \ll 1$, the above-threshold ionization (ATI) photoelectron distribution is consistent with the classical theory in which the photoelectron is forced only by the laser field after tunneling ionization [4], and the adiabatic condition applies [5]. In the multiphoton regime where $\gamma \gg 1$, the photoelectron spectrum (PES) consists of individual ATI peaks spaced by the energy of one photon [6,7]. In this regime, nonadiabatic effects will arise [1]. However, the mechanism of ionization is not clear around $\gamma \approx 1$ [8], which is the value of γ corresponding to most present experiments. In this region, the tunneling and multiphoton ionizations occur simultaneously, resulting in special characteristics. One of the most significant is nonadiabatic effects [9,10], meaning that the initial velocity offset of the electron at the tunnel exit is nonzero. In some certain special condition, the effects dominate the nonadiabatic tunneling and change the ionization rate. Nevertheless, many experiments interpret their results based on adiabatic theory; that is, the initial velocity of the ionized electron is zero. Is it justified to neglect nonadiabatic effects? This issue has no conclusive results at present [11–13]. In this work, we describe the effects by analyzing the initial velocity of the ionized electron.

Based on the pioneering Keldysh theory [5], which is known as strong-field approximation (SFA) [7,14], Perelomov, Popov, and Terent'ev (PPT) developed a method to obtain the ionization rate and momentum distribution [15]. Then Ammosov, Delone, and Krainov (ADK) [16] further summarized the PPT theory in the adiabatic tunneling limit in which electron tunneling is described as an adiabatic process.

Many previous experimental and theoretical works have been undertaken to investigate the nonadiabatic effects, and some contradictory conclusions were demonstrated. Arissian *et al.* [12] confirmed the validity of the adiabatic approximation by simulating the experimentally measured transverse momentum using an advanced ADK formula. In this condition, no photons are absorbed from the laser field and the initial velocity of the ionized electron is zero. Then Boge *et al.* [11] reported that the adiabatic theory is veracious to describe the experimental trends when $\gamma \leqslant 2.5$ by analyzing the deflection angle of the final momentum in laser field with different intensity. On the contrary, Shafir *et al.* [13] found that the initial velocity offset of the electron at the tunnel exit was nonzero, which contradicts the adiabatic theory. In addition, experiments [17] with a near-circularly-polarized laser have revealed ionization statistics incompatible with the adiabatic picture. Recently Mauger *et al.* [18] investigated the nonadiabatic effects through analyzing ionization rates and yields, and reported that nonadiabatic manifestations get stronger with increasing laser frequency.

In a linearly polarized laser pulse, the ionization process is complicated by the recollision process. The nonadiabatic effects are overwhelmed by other effects in rescattering, such as Coulomb focus [19]. However, in circularly polarized light, the ionized electron does not reencounter its parent ion and thus leads to a cleaner ionization signal. A circularly polarized laser pulse, which has now been introduced as a new powerful tool

*liuhongping@wipm.ac.cn

for investigating electron dynamics [20], has advantages for studying the ionization process. Some new phenomena, such as angular shifts in photoelectron momentum distributions [21], have also shown up in the circularly polarized laser field and have been investigated deeply [22,23].

In this work, we discuss the influence of wavelength on nonadiabatic effects in circularly polarized strong-field ionization by investigating the lateral angular distribution of PES, which is similar to the lateral momentum distribution studied in Refs. [12,24]. In addition, we integrate the angular distribution in a special range of the polar angle for clearly indicating nonadiabatic effects. We choose argon as the target atom exposed to circularly polarized pulses, because ionization of argon has been well documented in short-wavelength laser fields [25,26], which provides a benchmark for the present investigation. Here, we use the full quantum method based on solving the time-dependent Schrödinger equation (TDSE) in the length regime [27–29]. Hence, the PES can be easily obtained by simply projecting the electronic wave function onto the eigenstates of the field-free Hamiltonian at the end of the laser pulse.

II. THEORETICAL METHOD

The theoretical method has bean described in detail in our previous work [30] and here only a brief introduction is reviewed. We adopt the single-active-electron model to describe the dynamics of the argon atom in a strong laser field. In the model, the active electron is described by the TDSE as

$$i\frac{\partial}{\partial t}\psi(\mathbf{r},t)=\left[-\frac{\nabla^2}{2}+V^{(a)}(r)+V^{(\mathbf{F})}(\mathbf{r},t)\right]\psi(\mathbf{r},t), \quad (1)$$

where $V^{(a)}(r)$ represents the spherically symmetric three-dimensional potential of the atomic system and $V^{(\mathbf{F})}(\mathbf{r},t)=\mathbf{r}\cdot\mathbf{F}(t)$ is the laser-atom interaction under dipole approximation.

To solve the equation, we expand the time-dependent wave function in spherical coordinate $\mathbf{r}=(r,\theta,\phi)$ as [31]

$$\psi(\mathbf{r},t)=\sum_{l=0}^{l_{\max}}\sum_{m=-l}^{l}\frac{1}{r}\chi_{l,m}(r,t)Y_{l,m}(\theta,\phi), \quad (2)$$

where the reduced radial wave function $\chi_{l,m}(r,t)$ is represented in the sine-type discrete variable representation (sine-DVR) basis [32], and $Y_{l,m}(\theta,\phi)$ is the spherical harmonic. Based on this representation, we can benefit from angular momentum theory when dealing with the angular degrees of freedom.

We define the coordinate axis z parallel to the polarization vector of a linearly polarized electric field and then a set of coupled partial differential equations can be obtained,

$$i\frac{\partial}{\partial t}\chi_{l,m}(r,t)=\left[-\frac{1}{2}\frac{\partial^2}{\partial r^2}+\frac{l(l+1)}{2r^2}+V^{(a)}(r)\right]\chi_{l,m}(r,t) + rF(t)a_l\chi_{l+1,m}(r,t)+rF(t)a_{l-1}\chi_{l-1,m}(r,t), \quad (3)$$

with $a_l=\sqrt{(l+1)^2/(2l+1)(2l+3)}$. In this case, the azimuthal quantum number m is a conserved quantity. There is no transferred population among different m states. However, for the case in a circularly polarized field, m is not a conserved quantity any longer, and we introduce the Wigner rotation technique for solving the m-mixing problem so that the circularly polarized light is deemed to the rotation of linearly polarized light. In this way, we can treat the interaction of the electron with the nuclei and the field separately at each step of the time propagation. At the starting point in one propagation step, we represent the wave function in the atomic frame and calculate the action of electron-nuclei interaction operators, $-\frac{1}{2}\frac{\partial^2}{\partial r^2}$, $\frac{l(l+1)}{2r^2}$, and $V^{(a)}(r)$. Secondly, we transform the updated wave function to the laboratory fixed frame, where the polarization vector of the electric field is parallel to the z axis, with the Wigner rotation matrix $\mathbf{D}(\beta)$ by $\chi'(r_i,t)=\mathbf{D}(\beta)\chi(r_i,t)$, and then apply the obtained wave function to the electron-field interaction operator $V^{(F)}$. Finally, we transform the electronic wave function back by inverse rotation again to act on the electron-nuclei interaction operators. These operations make up a complete step of the time propagation. It should be noted that the Wigner rotation matrix is block diagonal with respect to l, allowing to perform the calculations very efficiently.

In the time propagation, the second-order split-operator scheme is employed, which is accurate and has been used widely [33–35]. In this scheme, one step of propagation is expressed as

$$\chi_{l,m}(t+\delta t)=e^{\frac{\delta t}{2}\frac{1}{2}\frac{\partial^2}{\partial r^2}}e^{-i\frac{\delta t}{2}\frac{l(l+1)}{2r^2}}e^{-i\frac{\delta t}{2}V^{(a)}(r)}e^{-i\delta tV^{(F)}}e^{-i\frac{\delta t}{2}V^{(a)}(r)}e^{-i\frac{\delta t}{2}\frac{l(l+1)}{2r^2}}e^{i\frac{\delta t}{2}\frac{1}{2}\frac{\partial^2}{\partial r^2}}\chi_{l,m}(t)+O(\delta t^3). \quad (4)$$

An exponential absorption potential is introduced in the propagation. Then through wave-packet propagation, the final reduced radial wave functions $\chi_{l,m}(r,t=T)$ can be obtained.

The PES is extracted by projecting the final wave function $\psi(\mathbf{r},t=T)$ onto the field-free wave function $\psi_E(r,\theta,\phi)=\sum_{l=0}^{l_{\max}}\sum_{m=-l}^{l}(1/r)\chi_{E,l}(r)Y_{l,m}(\theta,\phi)$, which is an eigenstate of the time-independent Hamiltonian at the energy E. A series of reduced radial eigenfunctions $\chi_{E,l}(r)$ are obtained by solving the time-independent Schrödinger equation by diagonalizing the field-free Hamiltonian. Therefore, the PES, which is a probability density, can be defined as follows [36]:

$$\begin{aligned}P(E)&=\left|\int_{r_{\min}}^{r_{\max}}\int_0^{\pi}\int_0^{2\pi}\psi_E^*(r,\theta,\phi)\psi(r,\theta,\phi,t=T)r^2\sin\theta dr d\theta d\phi\right|^2\\&=\sum_{l=0}^{l_{\max}}\sum_{m=-l}^{l}\left|\int_{r_{\min}}^{r_{\max}}\chi_{E,l}^*(r)\chi_{l,m}(r,t=T)dr\right|^2.\end{aligned} \quad (5)$$

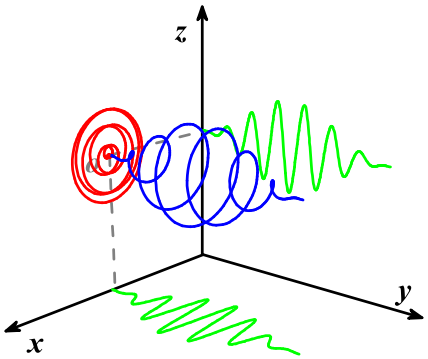

FIG. 1. (Color online) Schematic diagram of a circularly polarized laser pulse in a Cartesian coordinate system. The electric field oscillates in the xz plane ($\phi = 0$ or π in the spherical coordinate system) and the pulse propagates along the y axis.

Furthermore, the two-dimensional PES as a function of the kinetic energy and the polar angle at a constant azimuthal angle $\phi = \phi_0$ can be calculated as follows:

$$P(E,\theta) = \left| \int_{r_{\min}}^{r_{\max}} \psi_E^*(r,\theta,\phi_0)\psi(r,\theta,\phi_0,t = T)dr \right|^2. \quad (6)$$

Muller and Kooiman [37] and Tong and Lin [38] have given the three-dimensional atomic potential for the target argon atom, and both of the forms are accurate and used widely [39–41]. In our calculation, equidistant grids with 1509 points are used in the spatial r range of 0.0–400 a.u. The ground electronic state, corresponding to the ionization potential of 15.7 eV, is one of the eigenstates of the Hamiltonian in free field. Its corresponding wave function can also be obtained by the diagonalization mentioned above. We do not consider the influence of different magnetic quantum states, and the initial state is chosen to be the one of $m = 0$. The expansion in spherical harmonics is truncated at $l \leqslant l_{\max}$ ($l_{\max} = 50$ for wavelength $\leqslant 600$ nm, and $l_{\max} = 55$ for wavelength $=$ 800 nm). The convergent results can be obtained by checking the final PES for different truncations. A propagation time step of 0.02 a.u. is used. In this investigation, we choose the electric field with the form

$$F(t) = F_0 f(t) \begin{pmatrix} (\varepsilon/\sqrt{\varepsilon^2+1})\cos(\omega t + \varphi) \\ (1/\sqrt{\varepsilon^2+1})\sin(\omega t + \varphi) \\ 0 \end{pmatrix}, \quad (7)$$

where φ denotes the carrier-envelope phase; $\varepsilon = 1$ for the circular polarized pulse in this work; and the envelope $f(t) = \sin^2(\omega t/2N)$, with N the number of optical cycles. Here, we assume the pulse propagates along the y axis and the circularly polarized laser pulse oscillates in the xz plane in the Cartesian coordinate system as shown in Fig. 1; that is, $\theta = 0$ or π and $\varphi = 0$ or π in the spherical coordinate system.

III. RESULTS AND DISCUSSION

Figure 2 shows the temporal shape of the strong laser electric field applied [Fig. 2(a)] and the corresponding calculated results on the final photoelectron distribution [Figs. 2(b)–2(d)]. Here, the wavelength of the circularly polarized laser pulse equals 600 nm, the pulse duration is 7 cycles, and the peak top intensity equals 1.8×10^{14} W/cm^2. There is a main peak around the ponderomotive energy $U_p = 6.05$eV in the PES in Fig. 2(c), which means the ionization occurs in the tunneling regime [$U_p = F_0^2/(2\omega)^2$]. In addition, there are three small peaks (marked by the arrows), and the interval of these peaks is equal to the photon energy. Hence, there are tunneling and multiphoton ionizations simultaneously in this condition with the Keldysh parameter $\gamma = 1.61$. In order to image more clearly, the two-dimensional PES as a function of both the energy and polar angle is displayed in the plane (yz plane) perpendicular to the polarization plane, as shown in Fig. 2(b). There are obvious lateral distributions in the two-dimensional PES. In the directions at $\theta = 0$ and π, the two main peaks mean that the dominant ionization occurs in the tunneling regime when the adiabatic condition applies [5]. However, in the lateral distribution where the polar angle deviates away from the polarization plane, there are obvious multiphoton stripes which represent multiphoton ionization which occurs in the regime with $\gamma \gg 1$, and the nonadiabatic effects arise [1]. It is well known that the direction of final momentum of photoelectron is dependent on the polarization direction of laser field. However, the initial velocity direction of the ionized electron related to the nonadiabatic effects is isotropous. As the electric field vanishes in the lateral orientation (out of the xz plane or $\phi \neq 0$ and π) and there are no recollision electrons, any ionized electron which deviates from the polarization plane has lateral velocity. Thus, we can discuss the nonadiabatic effects by analyzing lateral distribution of photoelectrons. We integrated the two-dimensional PES over energy and analyzed the resulting one-dimensional angular distribution, as shown in Fig. 2(d). It clearly shows the lateral distribution of photoelectrons dependent on the polar angle.

We can compare the angular distribution of PES under different wavelength and laser intensity to understand the nonadiabatic effects. In Fig. 3, we plot the two-dimensional PES and the corresponding angular distribution in circularly polarized laser pulse with duration of 7 cycles and wavelength of 800 nm. In Figs. 3(a) and 3(b), the peak top intensity is the same as that used in Fig. 2 but the wavelength is longer. It is obvious that the lateral distribution of two-dimensional PES for 800-nm wavelength is weaker than that for 600-nm wavelength shown in Fig. 2(b), and the angular distribution is narrower than that in Fig. 2(d). In order to compare clearly, we define a special quantity, that is, the average lateral angle, which is defined as

$$\bar{\theta} = \frac{\int_0^{\pi/2} \theta P(\theta) d\theta}{\int_0^{\pi/2} P(\theta) d\theta}. \quad (8)$$

On account of the symmetry of the angular distribution on the z and y axes, as shown in Fig. 1, we integrate the angular distribution function in the range of $[0, \pi/2]$. The average lateral angles are equal to 19.25° and 27.6°, corresponding to the laser pulses of 800 and 600 nm, respectively. Thus, the influence of the nonadiabatic effect is important in the ionization process and nonadiabatic manifestations get stronger as the laser wavelength gets shorter.

The nonadiabatic effect is also influenced by field intensity. When the field intensity is reduced from 1.8×10^{14} to 1.0×10^{14} W/cm^2, the angular distribution gets broader, as shown

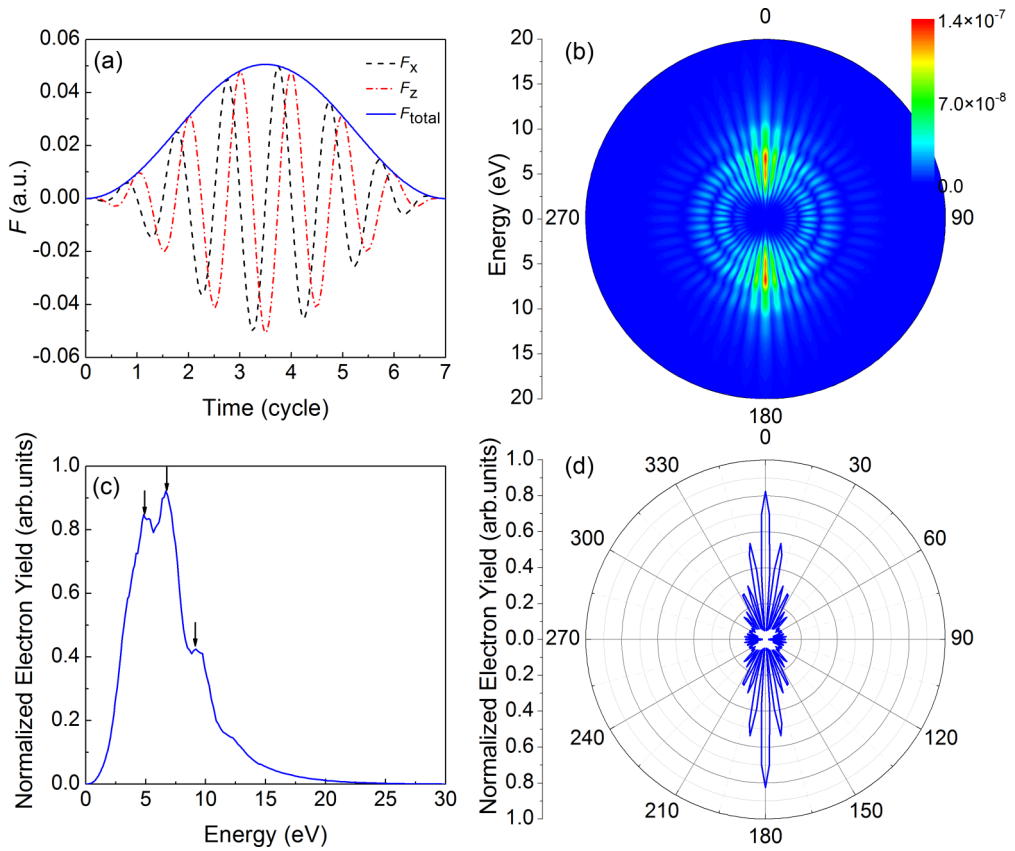

FIG. 2. (Color online) The electric-field envelope of circularly polarized laser (a) and the corresponding calculated results (b–d). The wavelength, pulse duration, and intensity are 600 nm, 7 cycles, and 1.8×10^{14} W/cm^2, respectively, corresponding to $\gamma = 1.61$.

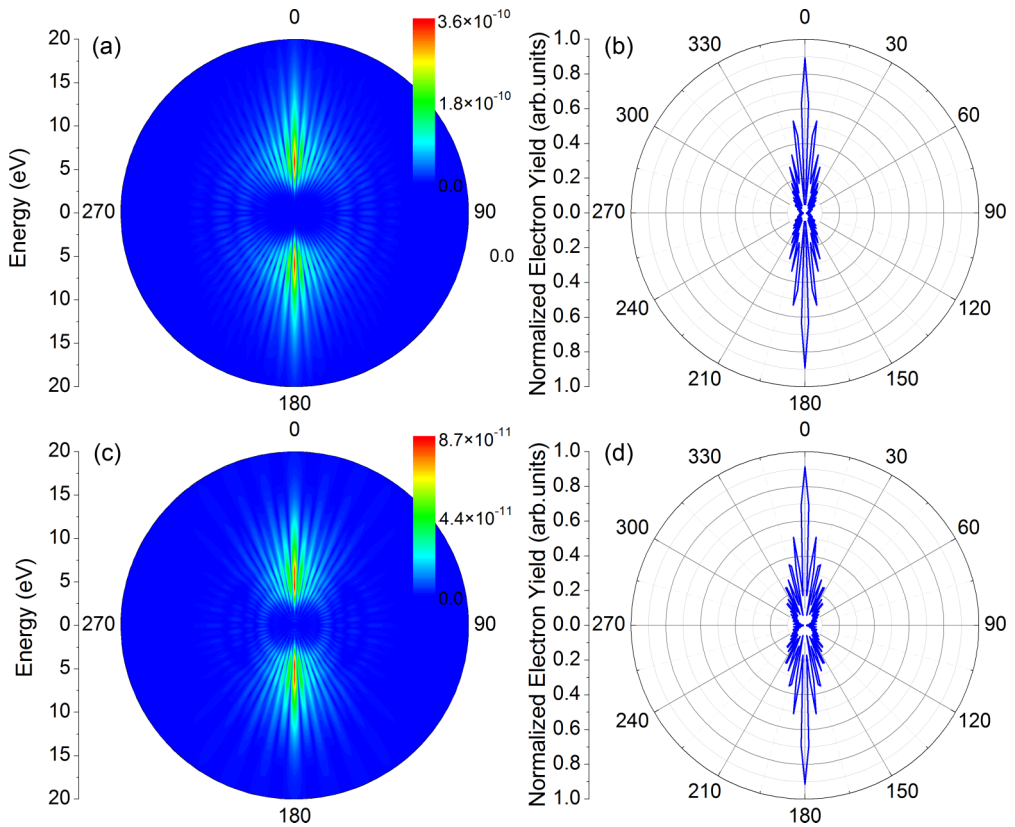

FIG. 3. (Color online) The two-dimensional PES and the corresponding angular distribution. The wavelength and pulse duration are 800 nm and 7 cycles, respectively. The laser intensities are 1.8×10^{14} W/cm^2 ($\gamma = 1.21$) (a,b) and 1.0×10^{14} W/cm^2 ($\gamma = 1.62$) (c,d).

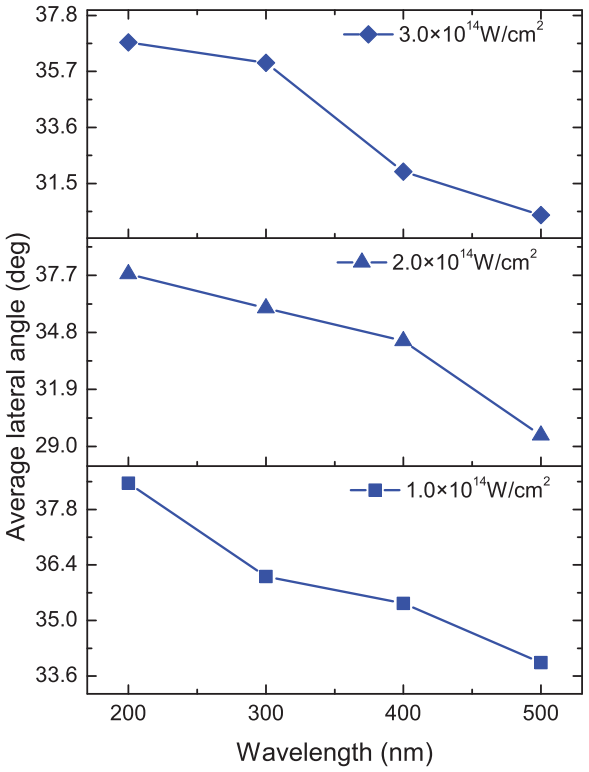

FIG. 4. (Color online) The curves of the average lateral angle as a function of wavelength. The circularly polarized laser pulses are taken as a duration of 9 cycles but with different intensities, 3.0×10^{14} W/cm^2 (upper), 2.0×10^{14} W/cm^2 (middle), and 1.0×10^{14} W/cm^2 (lower).

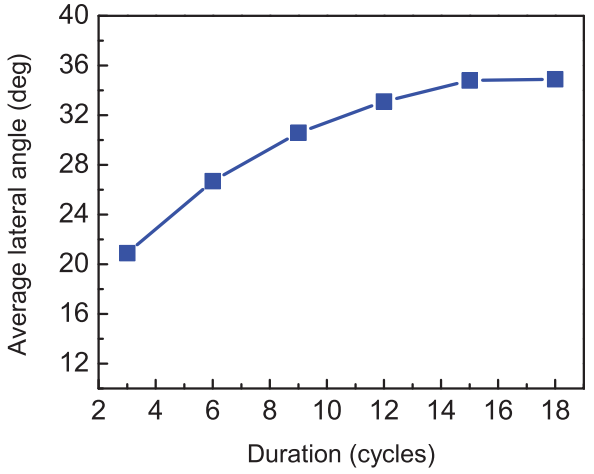

FIG. 5. (Color online) The curves of the average lateral angle as a function of duration in a 600-nm circularly polarized laser. The field intensity is 1.0×10^{14} W/cm^2 and the duration varies from 3 to 18 cycles.

in Figs. 3(c) and 3(d). Here the average lateral angle equals 23.87°, larger than the value of 19.25° obtained from Fig. 3(b). The phenomenon that the nonadiabatic effects increase in comparatively weaker laser fields can be explained with the time consumed in the ionization process. According to Keldysh time, $\Delta t = \sqrt{2I_{\rm ion}}/F$ [5], the ionization time is inversely proportional to the field intensity. This formally agrees with the well-known Büttiker-Landauer traversal time [42], which is a general definition that it would take for a photoelectron tunneling through the potential barrier with width of $I_{\rm ion}/F$. Thus, the ionization process needs more time in weaker fields.

In the region with large values of γ, the nonadiabatic effects are obvious, so we can study the influence of wavelength or intensity on the effects clearly. In Fig. 4, we plot the variation curve of the average lateral angle as a function of wavelength in a circularly polarized laser pulse with different intensities. The field intensities are taken to be 1.0×10^{14}, 2.0×10^{14}, and 3.0×10^{14} W/cm^2, respectively. The shortest and longest wavelengths are 200 and 500 nm, respectively. Thus, for these conditions, we can have the minimum value of Keldysh parameter of 1.50, where the ionization mainly occurs in the multiphoton regime. As is shown, the average lateral angle monotonically reduces with the wavelength increasing. It indicates that the nonadiabatic effects weaken in long wavelength. This is in accordance with the conclusion of Mauger and Bandrauk that nonadiabatic manifestations get stronger with increasing laser frequency [18]. Thus, the nonadiabatic effects are dominated by the time of the target atom exposed in the laser field. As is known, there are two time scales for a pulse, that is, a "slow" time scale related to the pulse envelope and a "fast" time scale corresponding to laser frequency or wavelength. In the calculation, all the laser pulses are chosen as the same value of 9 cycles; thus, the durations are unequal when the wavelength is different. Since both of the "slow" and "fast" time are changed, which is the real domination reason?

In Fig. 5, we calculate the average lateral angle in a circularly polarized laser pulse with the same wavelength but different durations. The wavelength and intensity take the same values, 600 nm and 1.0×10^{14} W/cm^2, respectively, and the range of the duration is 3–18 cycles. In these cases, the influence of wavelength vanishes and there is only a "slow" time scale effect. It is obvious that, as the number of cycles increases, the average lateral angle increases monotonically. This indicates that the nonadiabatic effects strengthen in a longer-duration laser pulse. In addition, there is another characteristic—that the increasing rate of the average lateral angle decreases with the increase of the laser pulse duration. That is, the increase of the average lateral angle is drastic in the range of short duration, whereas when the laser pulse is long enough, namely, more than 15 cycles in the calculation, the change of the average lateral angle almost disappears. That reminds us that the influence of altered pulse duration on the nonadiabatic effects is more obvious in a short-duration laser pulse than in a longer pulse. However, the nonadiabatic effects are stronger in a long-duration pulse, and the effects approach stabilization in a longer laser pulse. From the analysis of Fig. 4, we conclude that the "slow" time scale affects the nonadiabatic effects faintly, and when the time scale is "slow" enough (that is, the laser pulse is long enough), the nonadiabatic effects are invariant. Thus, the "fast" time dominates the nonadiabatic effects, and nonadiabatic effects will be stronger in a laser pulse with shorter wavelength.

IV. CONCLUSION

We have investigated the influence of wavelength on nonadiabatic effects in an intensive, circularly polarized laser field by solving TDSE of a single active electron in a three-dimensional spherical coordinate system. The two-dimensional PES as a function of both the energy and polar angle, and the corresponding angular distribution by integrating the two-dimensional PES over energy are calculated in the directions perpendicular to the polarization plane. Thus, the nonadiabatic effects can be manifested by the angular distribution. In order to study the nonadiabatic effects in laser pulses with different wavelengths, we calculate the average lateral angle by integrating the angular distribution function in the range of $[0, \pi/2]$.

In conclusion, in circularly polarized strong-field ionization when $\gamma \approx 1$, multiphoton ionization occurs in the lateral direction mainly where the nonadiabatic effects are expected to appear. By comparing the average lateral angles, we have shown that nonadiabatic effects are mostly dominated by the pulse wavelength and the effects get stronger for shorter wavelengths. In addition, the pulse duration also plays an important role on the nonadiabatic effects, but the influence on the nonadiabatic effects appears only in short pulses. When the duration is more than 15 cycles, the influence fades away and the nonadiabatic effects approach stabilization.

ACKNOWLEDGMENTS

We gratefully acknowledge L. B. Madsen for the help on the theoretical method and the valuable suggestions on the calculation in a circularly polarized laser. The work was supported by the China Postdoctoral Science Foundation (Grant No. 2015M572229), the National Key Basic Research Program of China (Grant No. 2013CB922003), and NSFC (Grants No. 11174329, No. 91121005, No. 91421305, and No. 11504412).

[1] M. Y. Ivanov, M. Spanner, and O. Smirnova, J. Mod. Opt. **52**, 165 (2005).
[2] P. B. Corkum, Phys. Rev. Lett. **71**, 1994 (1993).
[3] M. Abu-samha and L. B. Madsen, Phys. Rev. A **84**, 023411 (2011).
[4] H. B. van Linden van den Heuvell and H. G. Muller, *Multiphoton Processes* (Cambridge University, Cambridge, UK, 1988), where they give the name "simple-man" theory to this classical description.
[5] L. V. Keldysh, Zh. Eksp. Teor. Fiz. **47**, 1945 (1965) [Sov. Phys. JETP **20**, 1307 (1965)].
[6] P. Kruit, J. Kimman, H. G. Muller, and M. J. Van der Wiel, Phys. Rev. A **28**, 248 (1983).
[7] H. R. Reiss, Phys. Rev. A **22**, 1786 (1980).
[8] M. Yuan, D. Wang, J. Chen, A. Fu, F. Tian, and T. Chu, Can. J. Phys. **93**, 93 (2015).
[9] G. L. Yudin and M. Y. Ivanov, Phys. Rev. A **64**, 013409 (2001).
[10] I. Barth and O. Smirnova, Phys. Rev. A **84**, 063415 (2011).
[11] R. Boge, C. Cirelli, A. S. Landsman, S. Heuser, A. Ludwig, J. Maurer, M. Weger, L. Gallmann, and U. Keller, Phys. Rev. Lett. **111**, 103003 (2013).
[12] L. Arissian, C. Smeenk, F. Turner, C. Trallero, A. V. Sokolov, D. M. Villeneuve, A. Staudte, and P. B. Corkum, Phys. Rev. Lett. **105**, 133002 (2010).
[13] D. Shafir, H. Soifer, B. D. Bruner, M. Dagan, Y. Mairesse, S. Patchkovskii, M. Y. Ivanov, O. Smirnova, and N. Dudovich, Nature **485**, 343 (2012).
[14] F. H. M. Faisal, J. Phys. B: At. Mol. Opt. Phys. **6**, L89 (1973).
[15] A. M. Perelomov, V. S. Popov, and M. V. Terent'ev, Zh. Eksp. Teor. Fiz. **50**, 1393 (1966) [Sov. Phys. JETP **23**, 924 (1966)].
[16] M. V. Ammosov, N. B. Delone, and V. P. Krainov, Zh. Eksp. Teor. Fiz. **91**, 2008 (1986) [Sov. Phys. JETP **64**, 1191 (1986)].
[17] T. Herath, L. Yan, S. K. Lee, and W. Li, Phys. Rev. Lett. **109**, 043004 (2012).
[18] F. Mauger and A. D. Bandrauk, J. Phys. B **47**, 191001 (2014).
[19] D. Comtois, D. Zeidler, H. Pepin, J. C. Kieffer, D. M. Villeneuve, and P. B. Corkum, J. Phys. B **38**, 1923 (2005).
[20] X. Wang and J. H. Eberly, Phys. Rev. Lett. **105**, 083001 (2010).
[21] C. P. J. Martiny, M. Abu-Samha, and L. B. Madsen, J. Phys. B **42**, 161001 (2009).
[22] C. P. J. Martiny, M. Abu-samha, and L. B. Madsen, Phys. Rev. A **81**, 063418 (2010).
[23] C. P. J. Martiny and L. B. Madsen, Phys. Rev. Lett. **97**, 093001 (2006).
[24] I. Dreissigacker and M. Lein, Chem. Phys. **414**, 69 (2013).
[25] J. Wassaf, V. Véniard, R. Taïeb, and A. Maquet, Phys. Rev. Lett. **90**, 013003 (2003).
[26] L. Feng and T. Chu, Phys. Rev. A **84**, 053853 (2011).
[27] M. H. Yuan and T. S. Chu, Chem. Phys. **435**, 9 (2014).
[28] L. Feng and H. Liu, Commun. Comput. Chem. **2**, 47 (2014).
[29] L. Feng and T. S. Chu, Commun. Comput. Chem. **1**, 52 (2013).
[30] M. Yuan, R. Lü, L. Feng, and T. Chu, J. Chem. Phys. **140**, 074108 (2014).
[31] R.-F. Lu, P.-Y. Zhang, and K.-L. Han, Phys. Rev. E **77**, 066701 (2008).
[32] M. H. Beck, A. Jackle, G. A. Worth, and H. D. Meyer, Phys. Rep. **324**, 1 (2000).
[33] T.-S. Chu, Y. Zhang, and K.-L. Han, Int. Rev. Phys. Chem. **25**, 201 (2006).
[34] T. X. Xie, Y. Zhang, M. Y. Zhao, and K. L. Han, Phys. Chem. Chem. Phys. **5**, 2034 (2003).
[35] J. Hu, K.-L. Han, and G.-Z. He, Phys. Rev. Lett. **95**, 123001 (2005).
[36] X. Chen, A. Sanpera, and K. Burnett, Phys. Rev. A **51**, 4824 (1995).
[37] H. G. Muller and F. C. Kooiman, Phys. Rev. Lett. **81**, 1207 (1998).
[38] X. M. Tong and C. D. Lin, J. Phys. B **38**, 2593 (2005).
[39] H. G. Muller, Phys. Rev. A **60**, 1341 (1999).
[40] T. Morishita, Z. Chen, S. Watanabe, and C. D. Lin, Phys. Rev. A **75**, 023407 (2007).
[41] H. Wang, M. Chini, S. Chen, C.-H. Zhang, F. He, Y. Cheng, Y. Wu, U. Thumm, and Z. Chang, Phys. Rev. Lett. **105**, 143002 (2010).
[42] M. Büttiker and R. Landauer, Phys. Rev. Lett. **49**, 1739 (1982).